DOI: 10.1002/anie.201309077

Proton-Conducting Materials

Two-in-One: Inherent Anhydrous and Water-Assisted High Proton Conduction in a 3D Metal–Organic Framework**

*Sanjog S. Nagarkar, Sreekuttan M. Unni, Amitosh Sharma, Sreekumar Kurungot, and Sujit K. Ghosh**

Dedicated to Professor Susumu Kitagawa on the occasion of his 62nd birthday.

Abstract: *The development of solid-state proton-conducting materials with high conductivity that operate under both anhydrous and humidified conditions is currently of great interest in fuel-cell technology. A 3D metal–organic framework (MOF) with acid–base pairs in its coordination space that efficiently conducts protons under both anhydrous and humid conditions has now been developed. The anhydrous proton conductivity for this MOF is among the highest values that have been reported for MOF materials, whereas its water-assisted proton conductivity is comparable to that of the organic polymer Nafion, which is currently used for practical applications. Unlike other MOFs, which conduct protons either under anhydrous or humid conditions, this compound should represent a considerable advance in the development of efficient solid-state proton-conducting materials that work under both anhydrous and humid conditions.*

The increasing energy demands of the world in combination with limited natural resources have accelerated research in the field of alternative energy sources. Fuel cells seem to be an attractive option to improve energy, environmental, and economic security.[1,2] To increase the efficiency of fuel cells, materials that display a high proton conductivity ($0.1\ \mathrm{S\,cm^{-1}}$) and operate over a wide temperature range (25–300 °C) are required.[2] Today, most of the proton-conducting materials are based on Nafion, which works efficiently under humidified conditions and at lower temperatures (<80 °C). At elevated temperatures, however, the conductivity of Nafion drops significantly. Furthermore, the high cost associated with this membrane limits the wide-spread use of this material.[2a] Therefore, deliberate attempts are being made to develop efficient and inexpensive proton-conducting materials that operate over a wider temperature range.[3]

Metal–organic frameworks (MOFs) and coordination polymers (CPs) are well known for their high surface area and a designable structure with specific host–guest chemistry.[4] MOFs have been extensively investigated for storage, sensing, separation, catalysis, magnetism, and biomedical applications,[5] but only very recently, these solids have emerged as a new class of proton-conducting materials.[2] The facile fabrication of these materials, the feasibility of hybridization with other materials, their chemical stability, and conduction behavior make them suitable candidates for new solid-state proton-conducting materials.[6] As they are highly crystalline, MOFs may help us to understand the conduction mechanism and to optimize the ion conduction path. Proton-conducting MOF materials can be divided into two categories:[2,6] 1) water-assisted proton-conducting MOFs, which operate at low temperature (20–80 °C) and rely on the presence of water molecules and/or hydrogen-bonding interactions with water,[7] and 2) anhydrous proton-conducting MOFs, which work at intermediate temperatures (100–250 °C) by replacing water with amphiprotic organic molecules.[8] The MOFs that have been reported to date show high proton conductivity either under anhydrous conditions or in a humid environment.[2] Recently, Shimizu et al. highlighted the need for proton-conducting MOF materials that operate in both humid and anhydrous environments.[7m]

A couple of years ago, Kitagawa et al. reported rationally designed MOFs that are based on $\mathrm{Zn^{II}}$ and oxalate; in situ formed adipic acid molecules and the countercation $(\mathrm{NH_4})^+$ act as proton carriers with hydrogen-bonded water molecules.[7a] The compound shows high proton conduction under humidified conditions. But as for Nafion and other MOFs, the conductivity drops significantly with increasing temperature. Blends of polymers with free basic sites, such as amines, and strong acids ($\mathrm{H_2SO_4}$, $\mathrm{H_3PO_4}$) are known to form Brønsted acid–base pairs; proton transfer takes place in the absence of solvent (water) along hydrogen-bonded oxoacid anions and/or between the protonated and non-protonated basic sites under humid conditions and at elevated temperatures.[9] Thus, if we can maintain the hydrogen-bonded structure over a wider temperature range in the coordination space of porous materials, such as MOFs, efficient proton transport might become feasible both under humid conditions and at elevated temperatures in the solid state, as was observed for polymer blends.

Although MOFs can be engineered with some degree of certainty, a prediction of the type and the packing of guest molecules in the coordination space of MOFs is always

---

[*] S. S. Nagarkar, A. Sharma, Dr. S. K. Ghosh
Indian Institute of Science Education & Research (IISER)
Dr. Homi Bhabha Road, Pashan, Pune-411008 (India)
E-mail: sghosh@iiserpune.ac.in
Homepage: http://www.iiserpune.ac.in/~sghosh
S. M. Unni, Dr. S. Kurungot
Physical and Materials Chemistry Division
National Chemical Laboratory (NCL)
Dr. Homi Bhabha Road, Pashan, Pune-411008 (India)

[**] S.S.N. is thankful to CSIR for a research fellowship. We thank IISER, Pune for research facilities, and DST (GAP/DST/CHE-12-0083) and DAE (2011/20/37C/06/BRNS) for financial support.

Supporting information for this article is available on the WWW under http://dx.doi.org/10.1002/anie.201309077.

difficult. On the other hand, a large number of MOFs have been reported that can potentially be utilized for multiple applications, including proton conduction.[7b] Thus, an approach that makes use of the Cambridge Structural Database (CSD) is receiving increasing attention to find potential compounds with targeted properties.[7m,10] Using the CSD, we screened compounds for the presence of high-boiling proton carriers, higher carrier concentrations, the extent of hydrogen bonding, inexpensive starting materials, and ease of synthesis. An oxalate-based MOF $\{[(Me_2NH_2)_3(SO_4)]_2[M_2(ox)_3]\}_n$ (ox = oxalate) was found to be the most suitable candidate.[11] Using reported synthetic methods, a new three-dimensional MOF, namely $\{[(Me_2NH_2)_3(SO_4)]_2[Zn_2(ox)_3]\}_n$ (**1**) was synthesized solvothermally. The compound consists of an anionic framework $[Zn_2(ox)_3]^{2-}{}_n$ that is interpenetrated with a cationic supramolecular net $[(Me_2NH_2)_3SO_4]^{+}{}_n$, which is formed by electrostatic and hydrogen-bonding interactions between sulfate anions and dimethyl ammonium (DMA) cations. We then measured the anhydrous and water-assisted proton conduction in crystalline MOF **1**. The pure phase of **1** showed high proton conductivity under anhydrous conditions (1×10^{-4} S cm^{-1} at 150 °C), which is comparable or superior to the results obtained for other proton-conducting MOFs under similar conditions. Compound **1** also showed high water-assisted proton conductivity (4.2×10^{-2} S cm^{-1} at 98 % relative humidity (RH)), which is comparable to results obtained with Nafion.[2,7a] This is the highest proton conductivity that has been reported for MOF-based materials under similar conditions to date. In contrast to other MOFs, which perform either in humid or anhydrous conditions, the present compound is cheaper and shows high proton conductivity in humidified as well as anhydrous conditions. The features of this MOF, including a facile synthesis, inexpensive starting materials, and high proton conductivity, render it a suitable material for the development of solid-state proton-conducting materials that work in both humid and anhydrous conditions.

Compound **1** was synthesized solvothermally by reacting oxalic acid and $ZnSO_4\cdot7H_2O$ in dimethyl formamide (DMF). Single-crystal X-ray analysis of block-shaped crystals of **1** revealed that the compound crystallizes in the cubic system and the enantiomorphic $I4_132$ space group (Figure 1). The asymmetric unit of **1** consists of Zn^{2+} ions with 1/6 occupancy that are bound to oxalate with 1/4 occupancy giving rise to tris-chelated $[Zn_2(ox)_3]^{2-}$ subunits (Figure 1 a). The D_3-symmetric $[Zn_2(ox)_3]^{2-}$ subunit can be considered as a trigonally distorted octahedron. This anionic $[Zn_2(ox)_3]^{2-}{}_n$ net has 3D channels that were filled with dimethyl ammonium cations and disordered sulfate anions in the D_3 point group (Figure 1 b). The dimethyl ammonium cations are formed by decomposition of DMF in the presence of water. A sulfate ion from the metal salt binds to six dimethyl ammonium cations by electrostatic interactions and by 24 N−H···O hydrogen bonds to form a supramolecular $[(Me_2NH_2)_6SO_4]^{4+}$ cationic node, with NH···OS distances of 1.8–2.1 Å and N-H···O angles of 136.6–165.3° (Figure 1 c). The supramolecular cationic nodes $[(Me_2NH_2)_6SO_4]^{4+}$ are further connected to each other by electrostatic interactions and hydrogen bonding to form a 3D supramolecular $[(Me_2NH_2)_3SO_4]^{+}{}_n$ net (Figure 1 d). The overall structure of **1** can be visualized as an anionic net of $[Zn_2(ox)_3]^{2-}{}_n$ and a supramolecular cationic net of $[(Me_2NH_2)_3SO_4]^{+}{}_n$ that interpenetrate each other. As compound **1** crystallizes in a chiral space group with a flack parameter of 0.01, the solid-state circular dichroism spectrum of the bulk sample was recorded (Figure S1). No Cotton effect was observed for a bulk sample of **1**, which clearly indicates that both enantiomers are present in a 1:1 ratio.

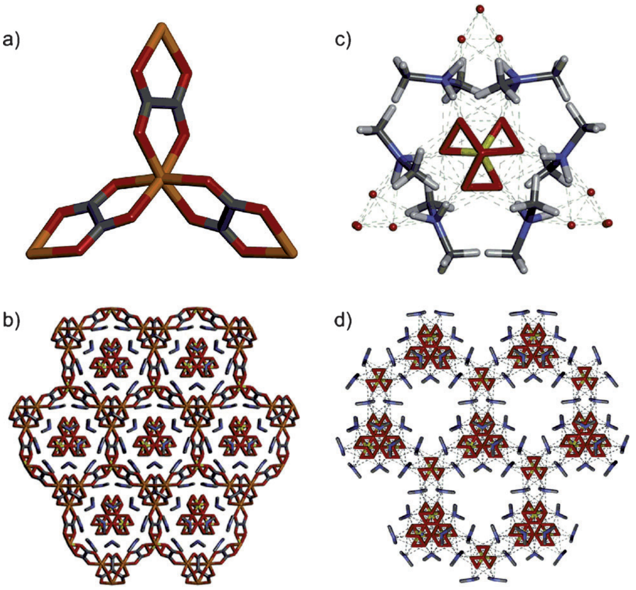

Figure 1. a) The tris-chelated D_3-symmetric $[Zn_2(ox)_3]^{2-}$ subunit. b) Crystal structure of $\{[(Me_2NH_2)_3(SO_4)]_2[Zn_2(ox)_3]\}_n$ (**1**). c) Hydrogen-bonding interactions between dimethyl ammonium cations and sulfate anions in compound **1**. d) 3D supramolecular $[(Me_2NH_2)_3SO_4]^{+}{}_n$ net formed by hydrogen bonding between dimethyl ammonium cations and sulfate anions. C gray, N blue, O red, S yellow, Zn orange. In Figure 1 b and d, H atoms are omitted for clarity.

The phase purity of the bulk sample was confirmed by matching the powder X-ray diffraction (PXRD) pattern of compound **1** and the PXRD pattern simulated from single-crystal analysis (Supporting Information, Figure S2). Thermogravimetric analysis of the polycrystalline sample under N_2 atmosphere revealed that the compound is stable up to 180 °C (Figure 2 a). The structural integrity of **1** towards higher temperatures was confirmed by overlapping the PXRD pattern of a sample of compound **1** that had been heated at 150 °C overnight and the PXRD pattern from the single-crystal structure (Figure S2). Variable-temperature PXRD analysis showed that the framework remains stable and highly crystalline during heating (30–150 °C) and cooling cycles (150–30 °C) without an alteration of the overall structure (Figure S3). To determine the stability of the compound **1** towards water, the compound was immersed in water overnight and the PXRD pattern was recorded upon drying. The overlapping PXRD patterns of as-synthesized and water-treated samples confirmed the water stability of this compound (Figure 2 b). The N_2 adsorption isotherm at 77 K revealed no uptake, which indicates the non-porous nature of the MOF towards gas, whereas the water sorption isotherm revealed an uptake of approximately 5 wt % (Figure S4).

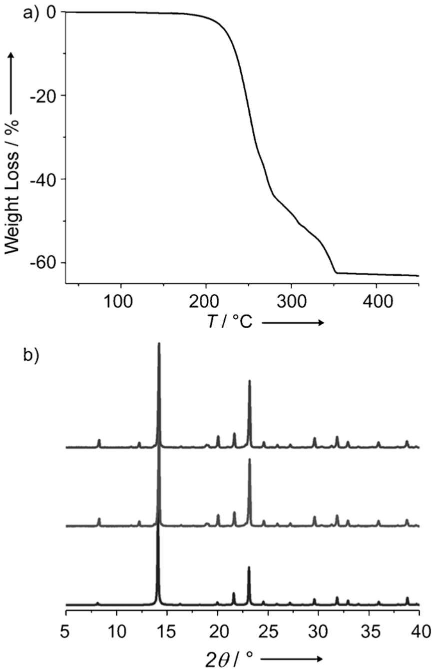

Figure 2. a) Thermogravimetric analysis of compound **1**. b) PXRD patterns of compound **1**; simulated pattern (bottom trace), as-synthesized (middle), and for a sample that was treated with water overnight (top).

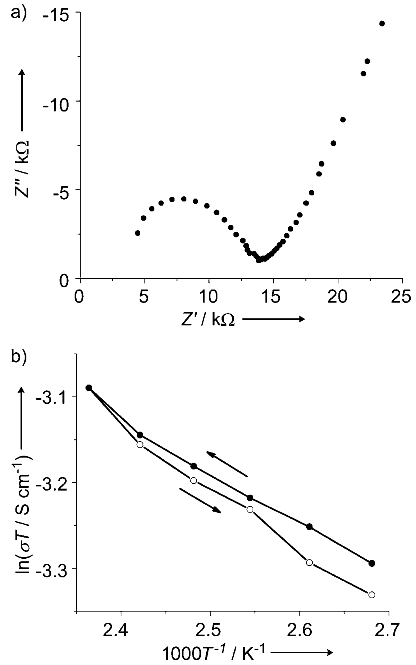

Figure 3. a) Impedance spectrum of compound **1** at 150 °C under anhydrous conditions. b) Arrhenius plot of **1** showing the dependence of anhydrous proton conductivity on temperature; heating cycle (●) and cooling cycle (○).

For efficient proton conduction, an extended hydrogen-bonded network is important. Single-crystal X-ray data reveals extensive 3D hydrogen bonding between DMA cations and sulfate anions. The IR spectrum of **1** also demonstrates the extensive hydrogen bonding between sulfate anions and dimethyl ammonium cations (Figure S5). The strong and broad peaks in the range of 3400–3500 cm^{-1} and at 2780 cm^{-1} can be ascribed to hydrogen-bonded N–H stretching vibrations, and the sharp peaks at 1000–1130 cm^{-1} are assigned to hydrogen-bonded sulfate anions.[11] The high thermal stability and the stability towards water, along with the extended 3D hydrogen-bonding network, makes **1** a potential candidate for proton-conducting materials under both humid and anhydrous conditions.

The proton conductivity of compound **1** was determined by alternating current (AC) impedance spectroscopy at 30 °C to 150 °C under anhydrous conditions. The real (Z′) and imaginary (Z″) parts of the impedance spectrum are shown in Figure 3 a. The semi-circle in the high-frequency region deals with bulk and grain boundary resistance, whereas the tail at low frequency corresponds to mobile ions that are blocked by the electrode–electrolyte interface. The proton conductivity for **1** was found to be $7\times10^{-5}\,S\,cm^{-1}$ at 30 °C under N_2 atmosphere. The conductivity increases with increasing temperature and reaches a maximum of $1.0\times10^{-4}\,S\,cm^{-1}$ at 150 °C (Figure 3 b). During the cooling cycle, the conductivity was found to decrease with decreasing temperature. The conductivity value of **1** at 150 °C under anhydrous conditions is among the highest conductivity values that have been reported for MOFs under anhydrous conditions; it is higher than those of imidazole-impregnated $[Al(\mu_2\text{-}OH)(1,4\text{-}ndc)]_n$ and $[Al(\mu_2\text{-}OH)(1,4\text{-}bdc)]$[8a] samples and comparable to those of β-PCMOF2,[8c] $[Zn(H_2PO_4)_2(TzH)_2]_n$[8f] and $[Zn(HPO_4)(H_2PO_4)_2](ImH_2)_2$ (1,4-bdc = 1,4-benzenedicarboxylic acid, 1,4-ndc = **1**,4-naphthalenedicarboxylic acid, Im = imidazole, Tz = triazole).[8e] Furthermore, as a step towards their application in fuel cells, we studied the time-dependent proton conductivity of **1** at 150 °C. Compound **1** showed high proton conductivity even after twelve hours with a negligible loss of conductivity (Figure 4). As temperature-dependent PXRD had shown that the structure does not change at 150 °C, the observed conduction behavior demonstrates the durability of the material, which is essential for practical applications.

To gain insight into the proton-conduction mechanism, we calculated the activation energy for **1** in both the heating and cooling cycles. The least-square fit of the Arrhenius plots for the heating and cooling cycles yielded very similar activation energy values (E_a) of 0.129 eV and 0.130 eV respectively, which are low enough to assume that the Grotthuss mechanism of proton conduction is operating.[2a,b] Furthermore, the activation value of **1** is the lowest value that has been reported

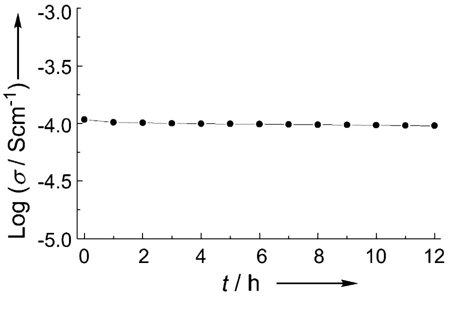

Figure 4. Time-dependent proton conductivity of **1** at T = 150 °C.

(total conduction) for MOF materials.[7m] The vehicle mechanism can be ruled out as the compound does not contain any species that transport protons over long ranges. Acid salts generally undergo a remarkable phase transition to the superprotonic state with an increase in proton conductivity of three-to-four orders of magnitude.[12] To detect the presence of any phase transition to the superprotonic state, we recorded the DSC profile of compound **1** at 25–180 °C (Figure S6). No phase transition was observed in the DSC profile, which ruled out the possibility of a transformation of **1** into a superprotonic phase. This hypothesis was further corroborated by the structural robustness that was observed during variable-temperature PXRD of **1**. As mentioned earlier, the proton conductivity is governed by the carrier concentration and the efficiency of the proton transport. We believe that as for polymer blends, the high proton conductivity of **1** originates from proton transfer along the hydrogen-bonded dimethyl ammonium cations and sulfate anions. Furthermore, because of in situ formation, uniform and high carrier loadings were obtained, which provide a continuous pathway for proton transport. Owing to the highly symmetric arrangement of proton carriers (cubic system), compound **1** conducts protons efficiently and isotropically, which leads to a high conductivity of the bulk sample.[13] Therefore, the highly symmetric and three-dimensionally ordered arrangement of proton carriers, along with strong and extensive hydrogen bonding in the supramolecular $[(Me_2NH_2)_3SO_4]^+_n$ net of **1**, yield fast and efficient proton transfer under anhydrous conditions in the bulk sample.

Low-temperature portable fuel cells are recently receiving increased attention as parts of power devices, including cellular phones and laptops.[2,14] We measured the conductivity of **1** at ambient temperature and under varying humidity. Impedance analysis of **1** under moderate humidity gave a good proton conductivity value of the order of 10^{-4} S cm^{-1} (Figure S7). To investigate the effect of water on the enhancement of proton conductivity of **1**, impedance analysis was performed with varying humidity in an incubator (Figure 5 a). At 30 % RH, the conductivity of **1** was found to be 4.4×10^{-5} S cm^{-1}, which further increased slowly with increasing humidity, and at 60 % RH, the conductivity increased to 1.4×10^{-3} S cm^{-1}. The conductivity reaches a maximum value of 4.2×10^{-2} S cm^{-1} at 98 % RH (Figure 5 b). It is noteworthy that this is the highest value that has been reported for any MOF-based proton-conducting materials that work under similar conditions to date.[2,6] The PXRD patterns before and after impedance analysis confirm the integrity of the compound during impedance analysis (Figure S8). Furthermore, reversible and retractable conduction behavior was observed during successive humidification cycles (Figures S9–11). The above data confirms that the conduction occurs because of the structure of the MOF and not because of dissolution.[7l]

The water adsorption isotherm shows a gradual uptake of water until 50 % RH, which is reflected by a small increase in water-assisted proton-conduction values. Above 50 % RH, the compound shows increased water uptake, which is in good agreement with the pronounced increase in the conductivity obtained for compound **1** above 50 % RH. We also measured the conductivity in the presence of D_2O, which gave a conductivity value of 3.7×10^{-2} S cm^{-1}, which is slightly lower than that of water as expected (Figure S12).

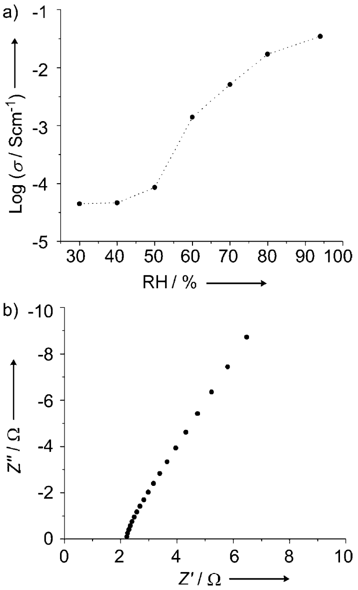

Figure 5. a) Dependence of the conductivity on humidity at 25 °C for **1** (••••• for reference). b) Impedance spectrum of compound **1** at 25 °C and 98 % RH.

The high proton conductivity under humidified conditions can be ascribed to the acid–base pair units, similar to those in polymer blends. The hydrophilic $(Me_2NH_2)^+$ cation is known to provide easily dissociable protons in the presence of water.[7h] Furthermore, the adsorbed water molecules can facilitate proton transfer to adjacent DMA cations through hydrogen bonding (Grotthuss mechanism) or as vehicles in the form of hydronium ions (vehicle mechanism).[7q] It is expected that these additional protons are efficiently transported by reforming hydrogen bonds between the sulfate anions and ammonium cations that are present in the supramolecular net, which gives rise to high proton conductivity. Also, a highly ordered carrier arrangement along with a high carrier concentration may support efficient proton transport. The mechanism is very similar to that described in a recent report by Kitagawa et al., in which the MOF contained free carboxylic acids with no lattice water.[7q] Under humid conditions, water serves as a mediator between adjacent carboxylate groups, which gives rise to efficient proton conduction. Such a cooperation between proton carriers and water for high conductivity has also been identified for $(NH_4)_2(adp)[Zn_2(ox)_3]\cdot H_2O$ (adp = adipic acid).[7a]

In our efforts to synthesize solid-state proton-conducting materials, we have reported a new 3D MOF that conducts protons under anhydrous as well as humidified conditions. The supramolecular net of acid–base pair units provides an efficient proton-conducting pathway under both conditions. The anhydrous proton conductivity of the present compound is comparable to that of MOF-based materials working under similar conditions. The water-assisted proton conductivity is comparable to that of Nafion and is the highest proton conductivity reported for MOF-based materials to date.

Unlike other MOFs, which perform only under humidified or anhydrous conditions, the present compound shows high proton conductivity under humidified as well as anhydrous conditions. Both inherent anhydrous and water-assisted high proton conduction make this MOF, which was synthesized from inexpensive starting materials, a significant material for further improvements of solid electrolytes and proton sensors.

Received: October 17, 2013
Published online: December 16, 2013

Keywords: conducting materials · fuel cells · metal–organic frameworks · porous materials · proton conduction

---

[1] a) R. F. Service, *Science* **2002**, *296*, 1222–1224; b) K. D. Kreuer, S. J. Paddison, E. Spohr, M. Schuster, *Chem. Rev.* **2004**, *104*, 4637–4678; c) H. Zhang, P. K. Shen, *Chem. Rev.* **2012**, *112*, 2780–2832; d) S. J. Peighambardoust, S. Rowshanzamir, M. Amjadi, *Int. J. Hydrogen Energy* **2010**, *35*, 9349–9384; e) M. Yoon, K. Suh, Y. Kim, N. Selvapalam, K. Kim, *Angew. Chem.* **2011**, *123*, 8016–8019; *Angew. Chem. Int. Ed.* **2011**, *50*, 7870–7873; f) P. Colomban, *Proton conductors, Solids, membranes and gels materials and devices*, Cambridge University Press, Cambridge, **1992**; g) C. Laberty-Robert, K. Valle, F. Pereira, C. Sanchez, *Chem. Soc. Rev.* **2011**, *40*, 961–1005; h) P. Tölle, C. Köhler, R. Marschall, M. Sharifi, M. Wark, T. Frauenheim, *Chem. Soc. Rev.* **2012**, *41*, 5143–5159; i) J. C. McKeen, Y. S. Yan, M. E. Davis, *Chem. Mater.* **2008**, *20*, 3791–3793; j) D. Basak, C. Versek, D. T. Toscano, S. Christensen, M. T. Touminen, D. Venkataraman, *Chem. Commun.* **2012**, *48*, 5922–5924.

[2] a) M. Yoon, K. Suh, S. Natarajan, K. Kim, *Angew. Chem.* **2013**, *125*, 2752–2764; *Angew. Chem. Int. Ed.* **2013**, *52*, 2688–2700; b) T. Yamada, K. Otsubo, R. Makiura, H. Kitagawa, *Chem. Soc. Rev.* **2013**, *42*, 6655–6669; c) S.-L. Li, Q. Xu, *Energy Environ. Sci.* **2013**, *6*, 1656–1683.

[3] a) M. Yamada, D. Li, I. Honma, H. Zhou, *J. Am. Chem. Soc.* **2005**, *127*, 13092–13093; b) M. Nogami, Y. Abe, *Phy. Rev. B* **1997**, *55*, 12108; c) M. T. Colomer, *Adv. Mater.* **2006**, *18*, 371; d) S. Fujita, A. Koiwai, M. Kawasumi, S. Inagaki, *Chem. Mater.* **2013**, *25*, 1584–1591.

[4] a) S. Kitagawa, R. Matsuda, *Coord. Chem. Rev.* **2007**, *251*, 2490–2509; b) O. M. Yaghi, M. O'Keeffe, N. W. Ockwig, H. K. Chae, M. Eddaoudi, J. Kim, *Nature* **2003**, *423*, 705–714.

[5] a) D. Zhao, S. T. Meek, J. A. Greathouse, M. D. Allendorf, *Adv. Mater.* **2011**, *23*, 249–267; b) J. J. Perry IV, J. A. Perman, M. Zaworotko, *J. Chem. Soc. Rev.* **2009**, *38*, 1400–1417; c) Y. Cui, Y. Yue, G. Qian, B. Chen, *Chem. Rev.* **2012**, *112*, 1126–1162; d) K. K. Tanabe, S. M. Cohen, *Chem. Soc. Rev.* **2011**, *40*, 498–519; e) S. S. Nagarkar, A. K. Chaudhari, S. K. Ghosh, *Cryst. Growth Des.* **2012**, *12*, 572–576; f) A. U. Czaja, N. Trukhan, U. Mueller, *Chem. Soc. Rev.* **2009**, *38*, 1284–1293; g) N. Stock, S. Biswas, *Chem. Rev.* **2012**, *112*, 933–969; h) S. S. Nagarkar, B. Joarder, A. K. Chaudhari, S. Mukherjee, S. K. Ghosh, *Angew. Chem.* **2013**, *125*, 2953–2957; *Angew. Chem. Int. Ed.* **2013**, *52*, 2881–2885; i) S. S. Nagarkar, A. K. Chaudhari, S. K. Ghosh, *Inorg. Chem.* **2012**, *51*, 572–576; j) R. J. Kuppler, D. J. Timmons, Q. R. Fang, J. R. Li, T. A. Makal, M. D. Young, D. Q. Yuan, D. Zhao, W. J. Zhuang, H. C. Zhou, *Coord. Chem. Rev.* **2009**, *253*, 3042–3066; k) B. Manna, A. K. Chaudhari, B. Joarder, A. Karmakar, S. K. Ghosh, *Angew. Chem.* **2013**, *125*, 1032–1036; *Angew. Chem. Int. Ed.* **2013**, *52*, 998–1002.

[6] S. Horike, D. Umeyama, S. Kitagawa, *Acc. Chem. Res.* **2013**, *46*, 2376–2384.

[7] a) M. Sadakiyo, T. Yamada, H. Kitagawa, *J. Am. Chem. Soc.* **2009**, *131*, 9906–9907; b) T. Yamada, M. Sadakiyo, H. Kitagawa, *J. Am. Chem. Soc.* **2009**, *131*, 3144–3145; c) T. Yamada, S. Morikawa, H. Kitagawa, *Bull. Chem. Soc. Jpn.* **2010**, *83*, 42–48; d) J. M. Taylor, R. K. Mah, I. L. Moudrakovski, C. I. Ratcliffe, R. Vaidhyanathan, G. K. H. Shimizu, *J. Am. Chem. Soc.* **2010**, *132*, 14055–14057; e) S. C. Sahoo, T. Kundu, R. Banerjee, *J. Am. Chem. Soc.* **2011**, *133*, 17950–17958; f) E. Pardo, C. Train, G. Gontard, K. Boubekeur, O. Fabelo, H. Liu, B. Dkhil, F. Lloret, K. Nakagawa, H. Tokoro, S. Ohkoshi, M. Verdaguer, *J. Am. Chem. Soc.* **2011**, *133*, 15328–15331; g) A. Shigematsu, T. Yamada, H. Kitagawa, *J. Am. Chem. Soc.* **2011**, *133*, 2034–2036; h) T. Panda, T. Kundu, R. Banerjee, *Chem. Commun.* **2013**, *49*, 6197–6199; i) R. M. P. Colodrero, K. E. Papathanasiou, N. Stavgianoudaki, P. Olivera-Pastor, E. R. Losilla, A. G. Aranda, L. Leon-Reina, J. Sanz, I. Sobrados, D. Choquesillo-Lazarte, J. M. Garcia-Ruiz, P. Atienzar, F. Rey, K. D. Demadis, A. Cabeza, *Chem. Mater.* **2012**, *24*, 3780–3792; j) F. Costantino, A. Donnadio, M. Casciola, *Inorg. Chem.* **2012**, *51*, 6992–7000; k) S. Sen, N. N. Nair, T. Yamada, H. Kitagawa, P. K. Bharadwaj, *J. Am. Chem. Soc.* **2012**, *134*, 19432–19437; l) S. R. Kim, K. W. Dawson, B. S. Gelfand, J. M. Taylor, G. K. H. Shimizu, *J. Am. Chem. Soc.* **2013**, *135*, 963–966; m) J. M. Taylor, K. W. Dawson, G. K. H. Shimizu, *J. Am. Chem. Soc.* **2013**, *135*, 1193–1196; n) N. C. Jeong, B. Samanta, C. Y. Lee, O. K. Farha, J. T. Hupp, *J. Am. Chem. Soc.* **2012**, *134*, 51–54; o) M. G. Goesten, J. Juan-Alcaniz, E. V. Ramos-Fernandez, K. B. S. S. Gupta, E. Stavitski, H. v. Bekkum, J. Gascon, F. Kapteijn, *J. Catal.* **2011**, *281*, 177–187; p) M. Sadakiyo, H. Okawa, A. Shigematsu, M. Ohba, T. Yamada, H. Kitagawa, *J. Am. Chem. Soc.* **2012**, *134*, 5472–5475; q) H. Okawa, M. Sadakiyo, T. Yamada, M. Maesato, M. Ohba, H. Kitagawa, *J. Am. Chem. Soc.* **2013**, *135*, 2256–2262.

[8] a) S. Bureekaew, S. Horike, M. Higuchi, M. Mizuno, T. Kawamura, D. Tanaka, N. Yanai, S. Kitagawa, *Nat. Mater.* **2009**, *8*, 831–836; b) D. Umeyama, S. Horike, M. Inukai, Y. Hijikata, S. Kitagawa, *Angew. Chem.* **2011**, *123*, 11910–11913; *Angew. Chem. Int. Ed.* **2011**, *50*, 11706–11709; c) J. A. Hurd, R. Vaidhyanathan, V. Thangadurai, C. I. Ratcliffe, I. L. Moudrakovski, G. K. H. Shimizu, *Nat. Chem.* **2009**, *1*, 705–710; d) V. G. Ponomareva, K. A. Kovalenko, A. P. Chupakhin, D. N. Dybtsev, E. S. Shutova, V. P. Fedin, *J. Am. Chem. Soc.* **2012**, *134*, 15640–15643; e) S. Horike, D. Umeyama, M. Inukai, T. Itakura, S. Kitagawa, *J. Am. Chem. Soc.* **2012**, *134*, 7612–7615; f) D. Umeyama, S. Horike, M. Inukai, T. Itakura, S. Kitagawa, *J. Am. Chem. Soc.* **2012**, *134*, 12780–12785.

[9] a) M. F. H. Schuster, W. H. Meyer, *Annu. Rev. Mater. Res.* **2003**, *33*, 233–261; b) T. Tezuka, K. Tadanaga, A. Hayashi, M. Tatsumisago, *J. Am. Chem. Soc.* **2006**, *128*, 16470–16471.

[10] a) E. Zass, D. A. Plattner, A. K. Beck, M. Neuburger, *Helv. Chim. Acta* **2002**, *85*, 4012; b) K. J. Msayib, D. Book, P. M. Budd, N. Chaukura, K. D. M. Harris, M. Helliwell, S. Tedds, A. Walton, J. E. Warren, M. Xu, N. B. McKeown, *Angew. Chem.* **2009**, *121*, 3323–3327; *Angew. Chem. Int. Ed.* **2009**, *48*, 3273–3277.

[11] C.-R. Li, S.-L. Li, X.-M. Zhang, *Cryst. Growth Des.* **2009**, *9*, 1702–1707.

[12] A. Goni-Urtiaga, D. Presvytes, K. Scott, *Int. J. Hydrogen Energy* **2012**, *37*, 3358–3372.

[13] Y. Chen, M. Thorn, S. Christensen, C. Versek, A. Poe, C. Hayward, M. T. Tuominen, S. Thayumanavan, *Nat. Chem.* **2010**, *2*, 503–508.

[14] S. Horike, Y. Kamitsubo, M. Inukai, T. Fukushima, D. Umeyama, T. Itakura, S. Kitagawa, *J. Am. Chem. Soc.* **2013**, *135*, 4612–4615.